Exophytic hepatocellular carcinoma, simulating a mesenchymal tumor, in a non-cirrhotic liver

Dear Editor,

A 26-year-old female presented with a five-month history of epigastric pain, nausea, and vomiting. She had recently lost weight (7 kg in the last month). Upon clinical examination, a bulky mass was palpated in the epigastric region.

Magnetic resonance imaging (MRI) (Figures 1A, 1B and 1C) revealed a solid, encapsulated, heterogeneous expansive mass in the epigastrium. The mass showed lobulated contours, measured approximately 25 × 20 × 12 cm, and had a volume of 3120 cm^3. Within the mass, which was compressing the body and tail of the pancreas, as well as the splenic vein, gastric fundus, and left lobe of the liver, there were foci of hyperintensity on T2-weighted images and hypointensity on T1-weighted images. The lesion presented discrete heterogeneous paramagnetic contrast enhancement. The results of laboratory tests, including alpha-fetoprotein levels, were within the limits of normality.

The patient underwent left lobe hepatectomy and resection of the neoplasm (Figure 1D). Pathological examination revealed a multifocal, Edmondson-Steiner grade II hepatocellular carcinoma, with macrotrabecular components, that was pseudoacinar and contained clear cells (moderately differentiated hepatocellular carcinoma).

Hepatocellular carcinoma is the most common primary tumor of the liver[1], although several other histological types have been reported[2–5]. Although hepatocellular carcinoma typically occurs in patients with liver cirrhosis, approximately 20% of cases occur in patients without it[6]. Its incidence peaks in the second and seventh decades of life, and it affects twice as many men as women[6]. Although hepatocellular carcinoma presents a variable aspect on MRI, it is typically hyperintense or isointense on T2-weighted images, whereas it is typically hypointense on T1-weighted images[7,8]. After administration of paramagnetic contrast, hepatocellular carcinoma presents intense enhancement in the arterial phase and hypointense signals in the portal and equilibrium phases, characterizing the contrast medium wash-out pattern[9]. Tumors larger than 1.5 cm typically present a fibrous capsule that appears as a hypointense band in the late phases[8,9]. Occasionally, hepatocellular carcinoma manifests as a large solitary mass[1,8].

Exophytic/pedunculated hepatocellular carcinoma is extremely rare[10]. One study showed that this type of tumor accounts for 0.24–3.0% of all cases of hepatocellular carcinoma in Japan[11]. It has an atypical presentation, manifesting as an extrahepatic mass in imaging studies, simulating another type of primary tumor[12]. In another study, there is a report of seven patients with extrahepatic masses seen on computed tomography, all simulating tumors of primary extrahepatic origin, in which the diagnosis of exophytic hepatocarcinoma was established only after percutaneous biopsy, surgical resection, or necropsy[13].

Here, we have presented the case of a patient who was young, had no history of liver disease or known risk factors for liver cirrhosis, had normal alpha-fetoprotein serum levels, and presented with a large epigastric mass that showed a hypovascular contrast pattern and was in contact with the liver. The main diagnoses considered were mesenteric sarcoma and an epithelioid gastrointestinal stromal tumor. In accordance with the findings of other studies, the diagnosis could not be made solely on the basis of the clinical data and MRI images obtained.

Exophytic hepatocellular carcinoma is difficult to diagnose. Therefore, when a bulky mass is discovered and is in contact with the surface of liver, this diagnostic possibility should be considered, even in patients who do not present risk factors for the condition[14].
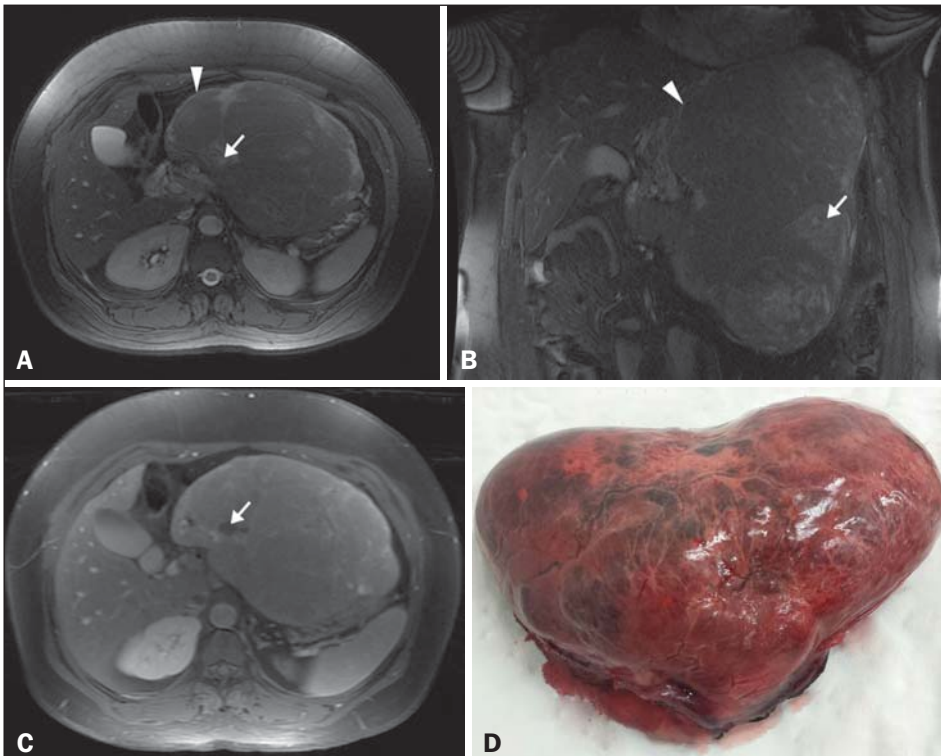

Figure 1. A,B: Axial and coronal fast imaging employing steady-state acquisition MRI with fat suppression. Solid, encapsulated, heterogeneous expansive mass in the epigastrium (arrowhead), with lobulated contours and areas of hyperintensity (arrow) consistent with necrosis. **C:** T1-weighted MRI acquisition with fat suppression after intravenous administration of paramagnetic contrast. Diffuse, heterogeneous paramagnetic contrast uptake by the neoplasm. Note the areas without uptake, which is consistent with necrosis (arrow). **D:** Macroscopic examination. Specimen received in formalin, designated as the product of a left hepatectomy, consisting of a liver fragment weighing 2354 g and measuring 23 × 17 × 11 cm, with an irregular shape, a smooth, brownish external surface, and a bloody area that measured 10 × 6 cm.

REFERENCES

1. Abou-Alfa GK, Jarnagin W, Lowery M, et al. Liver and bile duct cancer. In: Niederhuber JE, Armitage JO, Doroshow JH, et al., editors. Abeloff's clinical oncology. 5th ed. Philadelphia: Elsevier Saunders; 2014. p. 1373–96.

2. Szejnfeld D, Nunes TF, Fornazari VAV, et al. Transcatheter arterial embolization for unresectable symptomatic giant hepatic hemangiomas: single-center experience using a lipiodol-ethanol mixture. Radiol Bras. 2015;48:154–7.

3. Bormann RL, Rocha EL, Kierzenbaum ML, et al. The role of gadoxetic acid as a paramagnetic contrast medium in the characterization and detection of focal liver lesions: a review. Radiol Bras. 2015;48:43–51.

4. Candido PCM, Pereira IMF, Matos BA, et al. Giant pedunculated hemangioma of the liver. Radiol Bras. 2016;49:57–8.

5. Giardino A, Miller FH, Kalb B, et al. Hepatic epithelioid hemangioendothelioma: a report from three university centers. Radiol Bras. 2016; 49:288–94.

6. Gaddikeri S, McNeeley MF, Wang CL, et al. Hepatocellular carcinoma in the noncirrhotic liver. AJR Am J Roentgenol. 2014;203:W34–47.

7. Hennedige T, Venkatesh SK. Imaging of hepatocellular carcinoma: diagnosis, staging and treatment monitoring. Cancer Imaging. 2013; 12:530–47.

8. Chung YE, Park MS, Park YN, et al. Hepatocellular carcinoma variants: radiologic-pathologic correlation. AJR Am J Roentgenol. 2009; 193:W7–13.

9. Ros PR, Erturk SM, Malignant tumors of the liver. In: Gore RM, Levine MS, editors. Textbook of gastrointestinal radiology. 4th ed. Philadelphia: Elsevier Saunders; 2015. p. 1561–607.

10. Kimura H, Inoue T, Konishi K, et al. Hepatocellular carcinoma presenting as extrahepatic mass on computed tomography. J Gastroenterol. 1997;32:260–3.

11. Horie Y, Katoh S, Yoshida H, et al. Pedunculated hepatocellular carcinoma. Report of three cases and review of literature. Cancer. 1983;51: 746–51.

12. Roumanis PS, Bhargava P, Kimia-Aubin G, et al. Atypical magnetic resonance imaging findings in hepatocellular carcinoma. Curr Probl Diagn Radiol. 2015;44:237–45.

13. Longmaid HE 3rd, Seltzer SE, Costello P, et al. Hepatocellular carcinoma presenting as primary extrahepatic mass on CT. AJR Am J Roentgenol. 1986;146:1005–9.

14. Winston CB, Schwartz LH, Fong Y, et al. Hepatocellular carcinoma: MR imaging findings in cirrhotic livers and noncirrhotic livers. Radiology. 1999;210:75–9.

Glaucio Rodrigo Silva de Siqueira[1], Marcos Duarte Guimarães[2], Luiz Felipe Sias Franco[1], Rafaela Batista e Silva Coutinho[1], Edson Marchiori[3]

1. Hospital Heliópolis, São Paulo, SP, Brazil. 2. A.C.Camargo Cancer Center, São Paulo, SP, Brazil. 3. Universidade Federal do Rio de Janeiro (UFRJ), Rio de Janeiro, RJ, Brazil. Mailing address: Dr. Glaucio Rodrigo Silva de Siqueira. Rua Inácio Manuel Álvares, 1000, Bloco 2, ap. 24, Jardim Ester. São Paulo, SP, Brazil, 05372-111. E-mail: glauciosiqueira@yahoo.com.br.

Spondylometaphyseal dysplasia: an uncommon disease

Dear Editor,

A 2-year-old female patient, born by normal delivery, without complications, at 39 weeks of gestation, all prenatal test results having been normal, was referred to the department of orthopedics and traumatology for investigation of deformities of the thorax and ankle, as well as dwarfism. She showed no psychomotor alterations. The parents of the child were healthy, with no history of malformations, and the patient was their only child. They reported that the child had been born with dental precocity, with 9 teeth at birth, and began to present changes in the thorax and ankles at 4 months of age, those changes progressing thereafter. They also reported that the child had not grown, having been 75 cm tall since the age of 1 year and the same weight, approximately 9 kg, since the age 9 months, both of those measurements, according to the US CDC, being below the 5th percentile.

Physical examination of the patient showed a prominent sternum and shortening of the trunk, as well as discrete coxa vara with rotation to the right, flat feet, and deformity of the wrists (Figures 1A and 1B). On X-rays, we observed metaphyseal deformities such as bone rarefaction, aerated bone containing trabeculae, and cortical irregularity, as well as right-sided scoliosis and deformities of the ribs (Figures 1C and 1D). Using Todd's Atlas of Skeletal Maturation as a reference, we determined the bone age to be 21 months. Computed tomography scans (not shown) of the cervical spine and of the head, respectively, showed discrete hypoplasia of the odontoid process and a reduction in the amount white matter around the posterior horn of the lateral ventricles, neither of which have been reported in the literature.

Spondylometaphyseal dysplasia (SMD) was first described in 1967 by Kozlowski et al.[1], who defined it as a rare new form of bone dysplasia comprising various types of chondrodystrophy characterized by metaphyseal irregularities of the long bones, together with generalized platyspondyly of varying severity in the spine[1,2]. It produces a phenotypic spectrum of disorders, genotypically being autosomal dominant[3]. Kozlowski-type SMD, also known as type 1 SMD, is the most common form of the disease[1].

Figure 1. A,B: Physical examination showing a prominent sternum (**A**) and flat feet (**B**). **C,D:** X-rays showing platyspondyly and deformities of the ribs (**C**), as well as metaphyseal deformations such as bone rarefaction, aerated bone containing trabeculae, and cortical irregularity (**D**).